Polymer 50 (2009) 5871–5875

Contents lists available at ScienceDirect

Polymer

journal homepage: www.elsevier.com/locate/polymer

Polymer Communication

Polymer semicrystalline texture made by interplay of crystal growth

Yijin Ren [a], Liyun Zha [a], Yu Ma [a], Bingbing Hong [b], Feng Qiu [b], Wenbing Hu [a,*]

[a] Department of Polymer Science and Engineering, State Key Lab of Coordination Chemistry, School of Chemistry and Chemical Engineering, Nanjing University, 210093 Nanjing, China
[b] The Key Laboratory of Molecular Engineering of Polymers, Ministry of Education of China, Department of Macromolecular Science, Fudan University, 200433 Shanghai, China

ARTICLE INFO

Article history:
Received 12 September 2008
Received in revised form
22 March 2009
Accepted 18 September 2009
Available online 7 October 2009

Keywords:
Crystallization
Crystal growth
Crystallinity

ABSTRACT

Chain-folded lamellar crystal growth of polymers typically makes a semicrystalline texture, which exhibits a layer-by-layer, alternating assembly of crystalline and amorphous phases. We performed dynamic Monte Carlo simulations of lamellar crystal growth in a row structure. We found that parallel growth of lamellar crystals appears staggered at high temperatures, and those loops and cilia on the fold-end crystal surfaces interfere with the in-between lagging growth of the third crystal. This mechanism produces an intrinsic amorphous layer between two crystals, with its thickness comparable with coil sizes of single polymers. The results may facilitate our better understanding about the low crystallinity of high-molecular-weight polyethylenes, and the scaling law of their amorphous thickness on chain lengths.

1. Introduction

One significant characteristic of polymeric materials distinguished from other kinds of materials, such as highly crystalline metals and non-crystalline glassy oxides, is their semicrystalline texture. Semicrystalline polymers are strong because of the well-distributed lamellar crystals, and tough because of the interwoven highly elastic amorphous matrix. This mechanical feature of nano-composites nowadays endows their wide applications as most of engineering plastics and even some of commodity plastics. Therefore, understanding the semicrystalline texture is of essential importance in the study of polymer crystallization [1–3].

There are various factors controlling the crystallinity of polymers. The low crystallinity of statistical copolymers can be attributed to chemical, geometrical or stereo-optical irregularities in the sequential connections along the chain, which commonly behave as non-crystallizable co-units and segregate from the crystalline phases [4]. At low temperatures, when short regular sequences become crystallizable, the crystallinity of copolymers can be enhanced by the insertion mode of crystal growth in the amorphous region [5]. On the other hand, for homopolymers with a wide polydispersity of molecular weights, molecular segregation upon polymer crystal growth may also result in low crystallinity [6]. Besides the above segregation factors, the crystallographic frustration of α-form crystals of isotactic polypropylene (iPP) makes epitaxial branching that traps a lot of amorphous polymers in the compartment between crystallites [7], so the processing of iPP often demands for more β-form crystals to facilitate higher crystallinity. Very high crystallinity can be obtained in polyethylene (PE) by extended-chain crystal growth with extraordinarily high *c*-slip mobility in the hexagonal mesophase under high pressures [8].

Even if all the above-mentioned factors can be avoided, chain-folded crystal growth of polymers, nevertheless, always makes metastable semicrystalline textures [9]. This implies that the semicrystalline texture is an intrinsic result of chain-folded crystal growth. A typical example is again linear PE [10]. With the increase of molecular weights, the crystallinity of PE decreases under normal conditions [10] and the thickness of amorphous layers measured from the small-angle X-ray scattering (SAXS) exhibits a scaling law in its molecular-weight dependence [11].

In practice, the amorphous layer may contain free amorphous polymers, tie molecules connecting different crystals, loops connecting different sites of the same crystal, cilia connecting chain ends and the crystal, and dead entanglements of two loops belonging to separate crystals, etc. Recently, by means of molecular simulations, we observed the regime II–III transition in the temperature dependence of crystal growth rates, in company with a transition from single to multiple lamellar crystal growth at low temperatures [12]. We proposed that parallel growth of multiple

* Corresponding author.
E-mail address: wbhu@nju.edu.cn (W. Hu).

0032-3861/$ – see front matter © 2009 Elsevier Ltd. All rights reserved.
doi:10.1016/j.polymer.2009.09.073

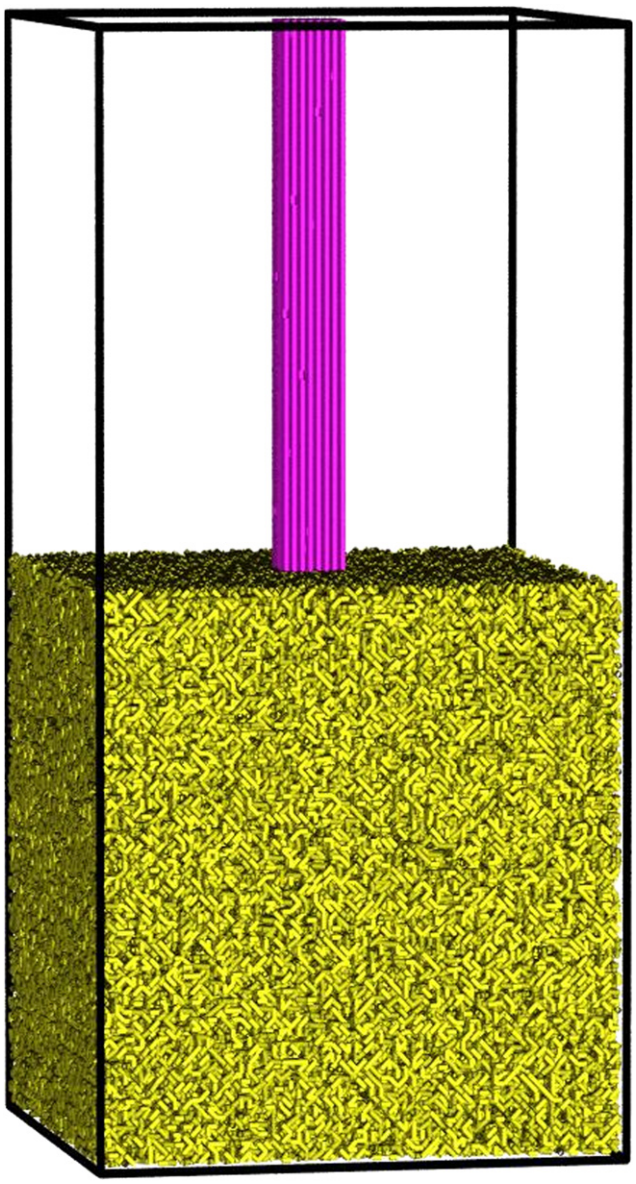

Fig. 1. Snapshot of the bulk amorphous 128-mers (shown in yellow) in $64 \times 64 \times 128$ cubic lattice with periodic boundary conditions [14]. 64 extended chains (shown in magenta) form an $8 \times 8 \times 128$ fiber to template crystal growth later. All the polymer bonds are drawn in tiny cylinders. Only half amorphous matrix is shown for clarity.

lamellar crystals will tighten up the slack part of tie molecules in the amorphous region between two neighboring crystals. Since the slack part is a prerequisite of polymers performing intramolecular secondary crystal nucleation at the crystal growth front [12], taut-tie molecules may prohibit any insertion growth of lamellar crystals in the amorphous layer. The question like which components can be responsible for the intrinsic amorphous layer is worthy of further investigations.

In this communication, we employed dynamic Monte Carlo simulations to demonstrate that those loops and cilia on the fold-end surfaces of lamellar crystals will block the insertion growth of crystals in the amorphous layer with its thickness comparable with coil sizes of single polymers. Such a mechanism of semi-crystalline texture is intrinsic in the interplay of polymer crystal growth and may explain why high-molecular-weight PE yields only low crystallinity and their amorphous thickness scales with chain lengths.

2. Simulation part

We simulated parallel growth of folded-chain lamellar crystals induced by the extended-chain fiber in a row structure. Such situation contains inherent information about polymer crystallization and self-assembly [13], for it commonly dominates the formation of both spherulites and shish-kebabs of polymer crystallites. In previous simulations, we have studied polymer crystal nucleation induced by the partial-molten single-species

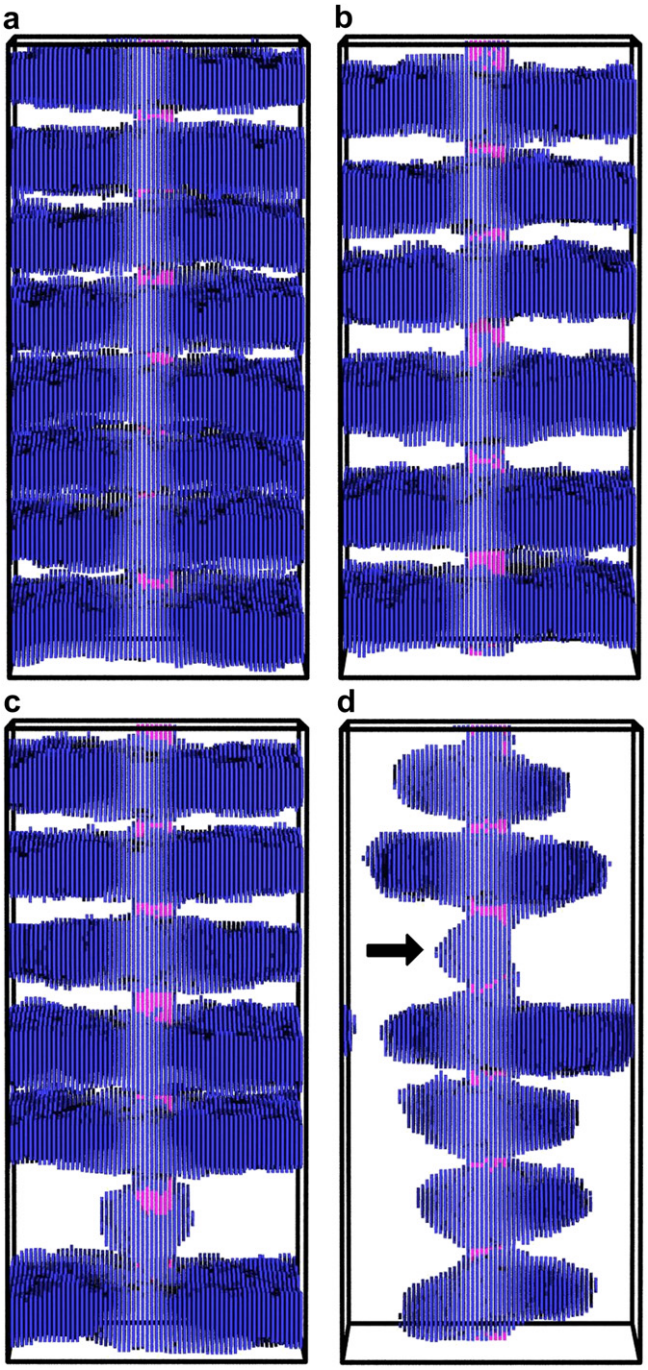

Fig. 2. Snapshots of crystallites grown from the central fiber under various temperatures. (a) $T = 5.0$ and time period 1.548×10^6 MC cycles; (b) $T = 5.2$ and time period 2.128×10^6 MC cycles; (c) $T = 5.3$ and time period 4.184×10^6 MC cycles; (d) $T = 5.35$ and time period 3.395×10^6 MC cycles. To expose crystallites, those bonds containing more than 10 parallel neighbors are drawn in blue tiny cylinders. The arrow in Fig. 2d indicates the region that will be carefully analyzed in Fig. 3.

fiber [14]. The initial state for inducing lamellar crystal growth in a row structure is shown in Fig. 1, where the central fiber is formed by immobile extended chains, and the occupation density of bulk polymers, each containing 128 monomers, is 0.9375 in the amorphous matrix. To eliminate the effect of chain-end defects in the central fiber, we randomly placed the extended chains along the fiber axis with periodic boundary conditions. Such an NVT simulation system assumes that any volume contraction upon crystallization will be dissipated right away, and only configurational information is retained.

We then quenched the initial sample system into variable low temperatures to observe the isothermal crystal growth induced by the central fiber. The conventional Metropolis sampling algorithm was employed to bias the micro-relaxation of lattice chains towards the crystalline state [15], with a potential energy barrier $E/kT = (pE_p + mE_c + \Sigma f_i E_f)/kT = (pE_p/E_c + m + \Sigma f_i E_f/E_c)E_c/kT$, where E_p was the parallel packing energy of two neighboring bonds to drive crystallization, E_c was the bending energy of two bonds along the chain to reflect chain flexibility, p and m were net amounts of nonparallel pairs of neighboring bonds, and of non-collinear connections of consecutive bonds along the chain, respectively; Σf_i was the sum of parallel neighbors along the path of local sliding diffusion, and E_f was the frictional barrier originated from the parallel neighbor of each bond in c-slip diffusion; k the Boltzmann constant and T the temperature. Introducing a frictional barrier for sliding diffusion will shift up the melting point, since such a barrier mainly exists in the crystalline region and will effectively stabilize the crystal. Similar effects have been observed in simulations of

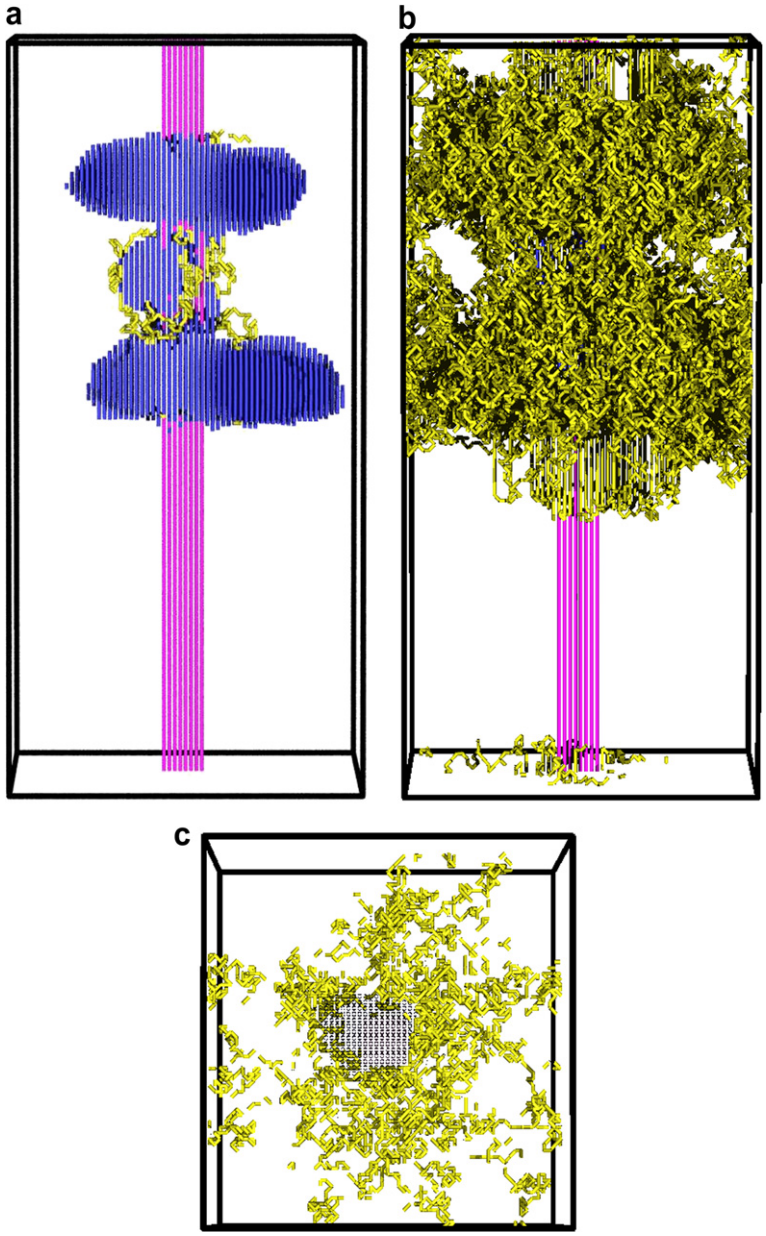

Fig. 3. a) Snapshot of the crystallites obtained at $T = 5.35$ and time period 2.943×10^6 MC cycles within the range between 60 and 112 along the fiber axis; tie molecules joining both top and bottom lamellar crystals are shown in yellow; (b) Snapshot of the crystallites same as in Fig. 3a; polymers joining either top or bottom lamellar crystals are shown in yellow; (c) Sectional view of the small in-between crystallite (section between 82 and 89 along the fiber axis); polymers joining either top or bottom lamellar crystals are shown in yellow. The crystalline bonds are defined as those containing more than 10 parallel neighbors. All the crystalline bonds are drawn in blue tiny cylinders.

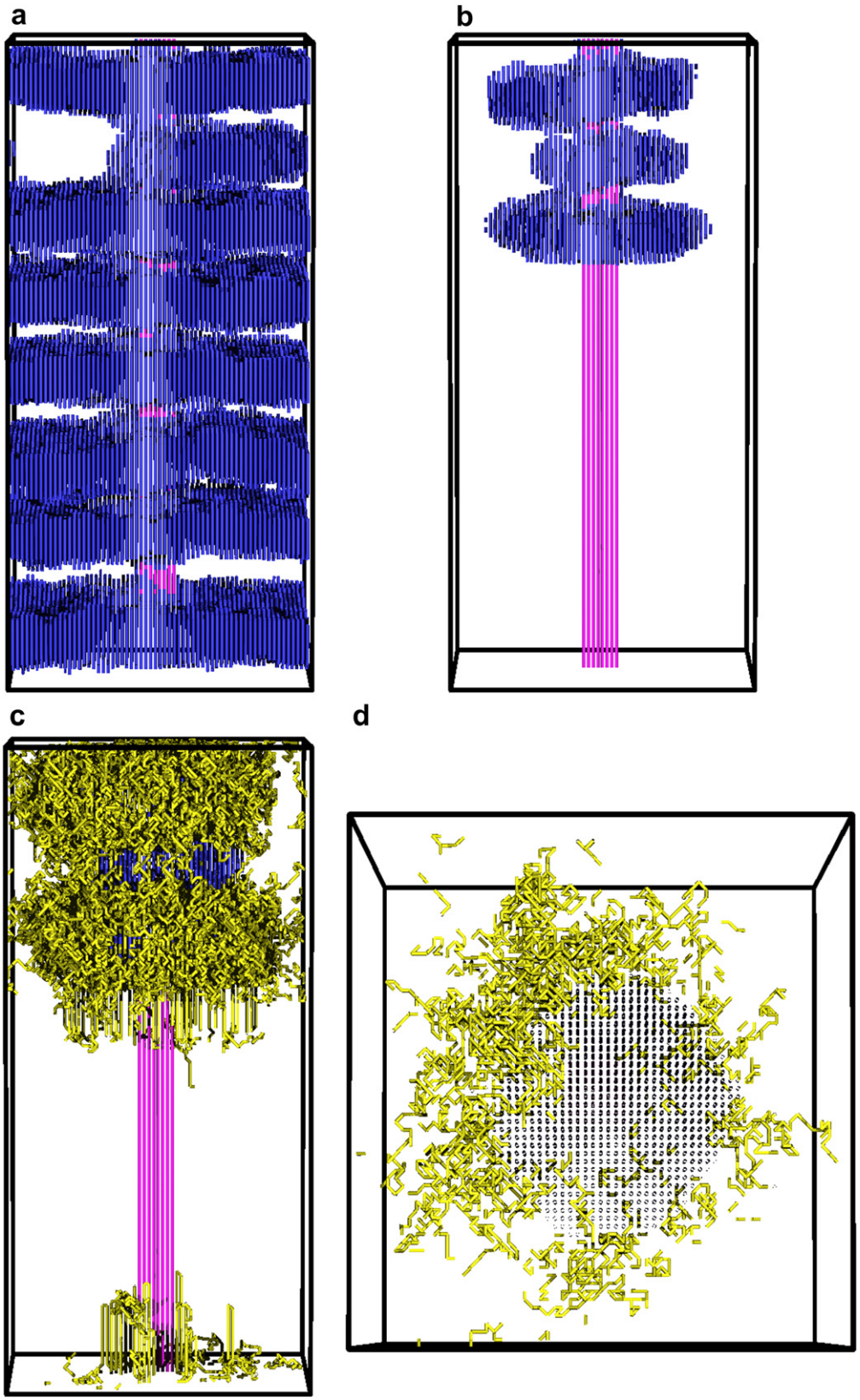

Fig. 4. a) Snapshot of the crystallites of 64-mers grown from the central fiber at $T = 5.15$ and time period 3.0×10^6 MC cycles; (b) Snapshot of the crystallites of 64-mers within the range between 85 and 115 along the central fiber, grown at $T = 5.15$ and time period 1.0×10^6 MC cycles; (c) Snapshot of the crystallites same as in Fig. 4b; polymers joining either top or bottom lamellar crystals are shown in yellow; d) Sectional view of the small in-between crystallite (section between 98 and 108 along the fiber axis); polymers joining either top or bottom lamellar crystals are shown in yellow. The crystalline bonds are defined as those containing more than 10 parallel neighbors, and are drawn in blue tiny cylinders.

crystallization and melting of statistical copolymers [16]. In practice, E_p/E_c was fixed at one to drive crystallization at temperatures where the chains were remained to be quite flexible; and E_f/E_c was fixed at 0.1 to avoid a large extent of crystal thickening right after crystal growth and thus to secure chain-folding without much further extending in the lamellar crystal. kT/E_c represents variable crystallization temperatures as simplified as T in the following text.

3. Results and discussion

As demonstrated in Fig. 2a–d, the density of lamellar crystals initiated from the central fiber decreases with the increase of temperatures, indicating a lowering efficiency of crystal nucleation. This temperature dependence is in accord with the common sense of crystal nucleation. The interesting point is that at high temperatures, when crystal nucleation becomes sporadic on the fiber, the profile of parallel growth of lamellar crystals appears staggered. One can see that growth of a crystal may lag behind its two neighbors and cannot grow mature into a large one, giving rise to a thick amorphous layer mainly responsible for a typical semicrystalline texture.

Why could the lagging lamellar crystal not grow mature in the thick amorphous layer between two parallel-growing crystals? The answer may provide us a key to understand the intrinsic semicrystalline texture on polymer crystallization. We therefore picked up the typical amorphous layer indicated by the arrow in Fig. 2d for detailed analysis. We did not observe any dead entanglements in this amorphous layer, as deduced from a simplified version of the topological analysis developed recently by Tzoumanekas and Theodorou [17]. This method detects the entanglement by shrinking single polymers with their two ends fixed till to the shrinking being blocked by topological constraints. On the other hand, we found a few tie molecules connecting both top and bottom lamellar crystals. In the snapshot of Fig. 3a, tie molecules were drawn in yellow. One can see that those tie molecules surround the in-between small crystal but may not be dense enough to interfere with its growth. If we go further to find out all those chains connecting either the top or the bottom lamellar crystals, i.e. those loops and cilia in the thick amorphous layer, as shown yellow in Fig. 3b, we will see that these chains are densely surrounding the in-between small crystal. A sectional view along the fiber axis, as shown in the snapshot of Fig. 3c, makes such a dense surrounding even more obvious.

Tie molecules are generated when two parallel-growing crystals are within a distance comparable with coil sizes of single polymers. To make sure that loops and cilia rather than tie molecules are responsible for the interference with the lagging crystal growth between two lamellar crystals. We cut all chain lengths (128-mers) into half (64-mers) and repeat the above simulation procedure for parallel growth. Fig. 4a demonstrates the staggered growth of parallel crystals at a high temperature for 64-mers. In this case, we focus our attention on the asymmetric amorphous layer generated in the top region of Fig. 4a. No more tie molecules can be found in the thick amorphous region, not mention the dead entanglements. Such an asymmetry actually occurs much earlier, as demonstrated in Fig. 4b, where the growth of the in-between crystal lags behind two neighboring crystals on the left-hand side, but its growth on the right-hand side still keeps shoulder to shoulder with its neighbors. Fig. 4c shows in yellow all those polymers joining either the top or the bottom crystals, exposing the asymmetric situation of loops and cilia surrounding the in-between crystal. Fig. 4d makes such an asymmetry even more obvious. The loops and cilia are much denser on the left-hand side than on the right-hand side, and thus block further growth of the in-between crystal towards the left-hand side.

Fig. 3c and Fig. 4d offer us a piece of direct visual evidence that loops and cilia can block the insertion growth of lamellar crystal in the amorphous layer. These loops and cilia are constrained by the connecting crystals and thus may not have enough lengths of the slack part of chains to perform intramolecular secondary crystal nucleation at the crystal growth front, like the previously proposed tie molecules and dead entanglements [12]. When the critical length of chain parts for nucleation becomes available at lower temperatures, insertion growth may occur again [5].

It should be emphasized that, in principle, those constrained part of chains between two neighboring lamellar crystals must be in the amorphous layer with its thickness comparable with the coil sizes of single polymers. This implies that the intrinsic amorphous thickness is correlated with chain lengths, and thus explains why the amorphous thickness scales with chain lengths [10] as well as why those high-molecular-weight polymers make only low crystallinity [11].

4. Conclusion

In summary, we performed molecular visualization to demonstrate a piece of evidence on how the lagging crystal growth can be blocked in the amorphous region between two neighboring crystals. Those loops and cilia, both constrained by two neighboring lamellar crystals within a distance comparable with the coil sizes of amorphous polymers, are responsible for this behavior. Such a result expands our previous proposition for those components interfering with insertion growth of lamellar crystals from tie molecules and dead entanglements to constrained loops and cilia.

Here, asynchronous growth of lamellar crystals can be assigned to sporadic crystal nucleation on the fiber seed at high temperatures. More general staggering profile exists at the frontier of polymer spherulites where parallel growth is initiated by continuing small-angle branching of lamellar crystals, for instance, in a way like screw dislocation, which results in an intrinsic semicrystalline texture under even low temperatures. Such an intrinsic semicrystalline texture may explain the experimental facts that high-molecular-weight polymers harvest only low crystallinity and their amorphous thickness scale with chain lengths.

Acknowledgements

WH thanks stimulating discussions from Prof. Shouke Yan at Beijing University of Chemical Technology and appreciates the financial support from National Natural Science Foundation of China (NSFC Grant No. 20674036 and 20825415). FQ acknowledges the support from the National Basic Research Program of China (Grant No. 2005CB623800).

References

[1] Wunderlich B. Macromolecular physics, vol. 1–3. New York: Academic Press; 1973, 1976, 1980.
[2] Bassett DC. Principles of polymer morphology. London: Cambridge University Press; 1981.
[3] Mandelkern L. Crystallization of polymers. In: Kinetics and mechanisms, vol. 2. London: Cambridge University Press; 2004.
[4] Hu WB, Mathot VBF, Frenkel D. Macromolecules 2003;36:2165.
[5] Strobl G. The physics of polymers. Berlin, Hedelberg: Springer-Verleg; 2007. p208.
[6] Hu WB. Macromolecules 2005;38:8712.
[7] Lotz B, Wittman JC, Lovinger AJ. Polymer 1996;37:4979.
[8] Wunderlich B, Davidson T. J Polym Sci Part-A2: Polym Phys 1969;7:2043.
[9] Keller A, Cheng SZD. Polymer 1998;39:4461.
[10] Mandelkern L. Acc Chem Res 1990;23:380.
[11] Robelin-Souffache E, Rault J. Macromolecules 1989;22:3581.
[12] Hu WB, Cai T. Macromolecules 2008;41:2049.
[13] Bassett DC. Polymer 2006;47:5221.
[14] Cheng SJ, Hu WB, Ma Y, Yan SK. Polymer 2007;48:4264.
[15] Hu WB, Frenkel D. Adv Polym Sci 2005;191:1. See the Appendix for more details of simulation techniques.
[16] Hu WB, Karssenberg FG, Mathot VBF. Polymer 2006;47:5582.
[17] Tzoumanekas C, Theodorou DN. Macromolecules 2006;39:4592.